Canadian Journal of
pure&applied
sciences

DISCRIMINATION OF MULTIDRUG RESISTANCE IN DIFFERENT OVARIAN CANCER CELLS USING A SINGLE-CELL BIOANALYZER

Haiyan Wang[1,2], Avid Khamenehfar[2], Michael Chung Kay Wong[2,4], James Lian Zhong Wang[4], *Paul Chi Hang Li[2,5],
Da Zhou[3], Marinko Sarunic[3], Feng Feng[1], Hairong Cao[1] and King Leung Fung[5]

[1]Department of Chemistry and Environmental Engineering, Shanxi Datong University, Datong, Shanxi, China
[2]Department of Chemistry, Simon Fraser University, Burnaby, British Columbia
[3]School of Engineering, Simon Fraser University, Burnaby, British Columbia, Canada
[4]ZellChip Technologies Inc. Burnaby, British Columbia, Canada
[5]Laboratory of Cell Biology, Center for Cancer Research, National Cancer Institute,
National Institutes of Health, Bethesda, Maryland, USA

ABSTRACT

A single-cell bioanalyzer (SCB) was presented to detect different ovarian cancer cells, i.e. to discriminate NCI/ADR-RES cells, which are multidrug resistant (MDR), from non-MDR OVCAR-8 cells. This discrimination has been achieved in the single-cell level by measuring drug accumulation in real-time, in which the accumulation is high in non-MDR single-cells without drug efflux, but is low in MDR single-cells with efflux. The SCB was constructed as an inverted microscope for optical imaging and fluorescence measurement of a cell that was retained in a microfluidic chip. The cell retained in the chip offers sufficient fluorescence signals for the SCB to measure the accumulation of daunorubicin (DNR) in a single ovarian cancer cell in the absence of the MDR inhibitor, cyclosporine A (CsA). The same cell allows us to detect the enhanced drug accumulation due to MDR modulation in the presence of CsA. The measurement of drug accumulation in a cell was achieved after it was captured in the chip, with the correction of background interference. The detection of accumulation enhancement due to MDR modulation by CsA was determined in terms of either the accumulation rate or enhanced amount of DNR in the same single-cell. It showed that with the effectiveness of efflux-blocking by CsA, DNR in a single-cell was increased by 3-fold against its same-cell control. For this single-cell bioanalyzer (SCB), it has the ability to discriminate MDR in different ovarian cells due to drug efflux in them by eliminating the interference of background fluorescence and by using the same-cell control.

Keywords: Single cell bioanalyzer, optical imaging, fluorescence measurement, microfluidic chip, same-cell control, multidrug resistance.

INTRODUCTION

It was proposed that highly integrated microdevices or microchips show great promise for basic biomedical and pharmaceutical research, and robust point-of-care devices could be developed for use in clinical settings (El-Ali *et al*., 2006). Since then, the microfluidic chip, which can be designed to contain features compatible with the size of human cells, has been used for the study of cell biology and analysis (Gómez-Sjöberg *et al*., 2007; Halldorsson *et al*., 2015; Lindström *et al*., 2010). Cell studies using microfluidic devices require low numbers of cell population down to a few hundred cells, or even a few cells, making it possible to measure perturbations of individual cells, increasing the spatial and temporal resolutions of the measurements for a given experimental

setup. In 2008, the concept of same-single-cell analysis (SASCA) was proposed (Li *et al*., 2008), and the method was developed for the study of multidrug resistance (MDR) and its modulation in MDR cancer cells using real-time monitoring of drug efflux (Li *et al*., 2008), or of drug accumulation (Li *et al*., 2011), with the latter mode dubbed SASCA-A. Recently, this SASCA-A method was employed to measure drug accumulation and overcome MDR in murine melanoma B160VA cells (Khamenehfar *et al*., 2014a), human prostate 22Rv1 cells (Khamenehfar *et al*., 2015a), human leukemia patient cells (Khamenehfar *et al*., 2016) and non-small cell lung cancer H1650 cells (Khamenehfar *et al*., 2015b). In addition, to enhance drug accumulation, the SASCA method was used to identify various MDR modulators, such as the low-molecular-weight diblock copolymer, (Khamenehfar *et al*., 2014b), and ginsenosides (Chen *et al*., 2014).

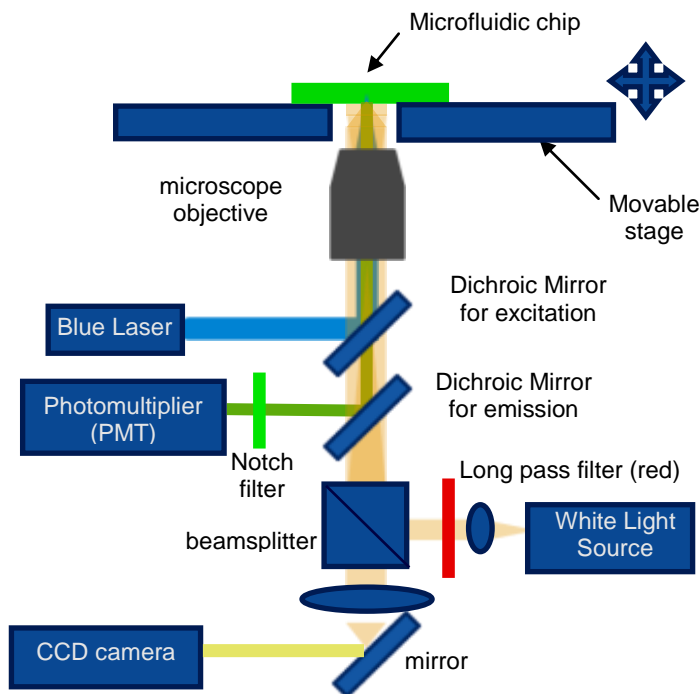
*Corresponding author e-mail: paulli@sfu.ca

Fig. 1. Schematic diagram of the microscope-based single-cell bioanalyzer (SCB). The *microfluidic chip* is placed on a *movable stage*. There are 3 optical paths for the SCB conducting simultaneous optical imaging and fluorescence measurement of single-cells. The blue path represents the fluorescence excitation light provided by the *blue laser* and reflected on the *dichroic mirror for excitation* to pass through the *microscope objective* to excite drug molecules in a single-cell captured in the *chip*. The green path represents the fluorescence emitted from the drug molecules, which passed through the *microscope objective* and reflected on the *dichroic mirror for emission* to reach the *photomultiplier tube (PMT)* via a green *notch filter* for fluorescence measurement. The yellow path represents the red-colored light provided by the *white light source* and *long-pass filter* reflected on the *beam splitter* to the *chip*; then from the *chip* back and reflected on the *mirror* to the *CCD camera* for optical imaging.

In this study, the single cell bioanalyzer (SCB), which is an inexpensive and sensitive optical imaging/fluorescence measurement system, has been developed to measure multidrug resistance (MDR) in ovarian cells, discriminating the drug accumulation in these cells by using and not using cyclosporine A (CsA). A schematic diagram of the microscope-based imaging/measurement system of SCB is depicted in Figure 1. With the deduction of background fluorescence interferences accomplished by a previously reported method (Peng and Li, 2005), the corrected cellular fluorescence signals significantly distinguish drug accumulation between the test cell and its "same-cell control" in a convenient and fast manner. The optical parts and electronic components in the SCB are assembled with the mechanical parts that are fabricated in plastics by a 3-D printer, as depicted in Figure 2.

In terms of MDR, it is known that the permeability-glycoprotein (P-gp), a 170-kDa transmembrane drug transporter protein located in the cell membrane, plays a major role in cellular MDR (Sharom *et al*., 2008). This is resulted via the efflux of different classes of chemotherapeutic agents or drugs, lowering the accumulation of drugs in the cancer cells and hence reducing the effectiveness of chemotherapy (Thomas and Coley, 2003; Li *et al*., 2016). Cyclosporine A (CsA), which typically inhibits P-gp by interacting with its drug-binding domain (Marquez and Van Bambek, 2011), has been selected to enhance the accumulation of P-gp substrates in cancer cells in our experiments.

Using the single-cell bioanalyzer (SCB), we measured drug accumulation in the drug-resistant ovarian carcinoma cells (NCI/ADR-RES) and its parental control (OVCAR-8) quantitatively in a one hour time-frame. The electronic signals that are related to the fluorescence intensities of the single cancer cells significantly distinguish between two lines of ovarian cells, and by this real time
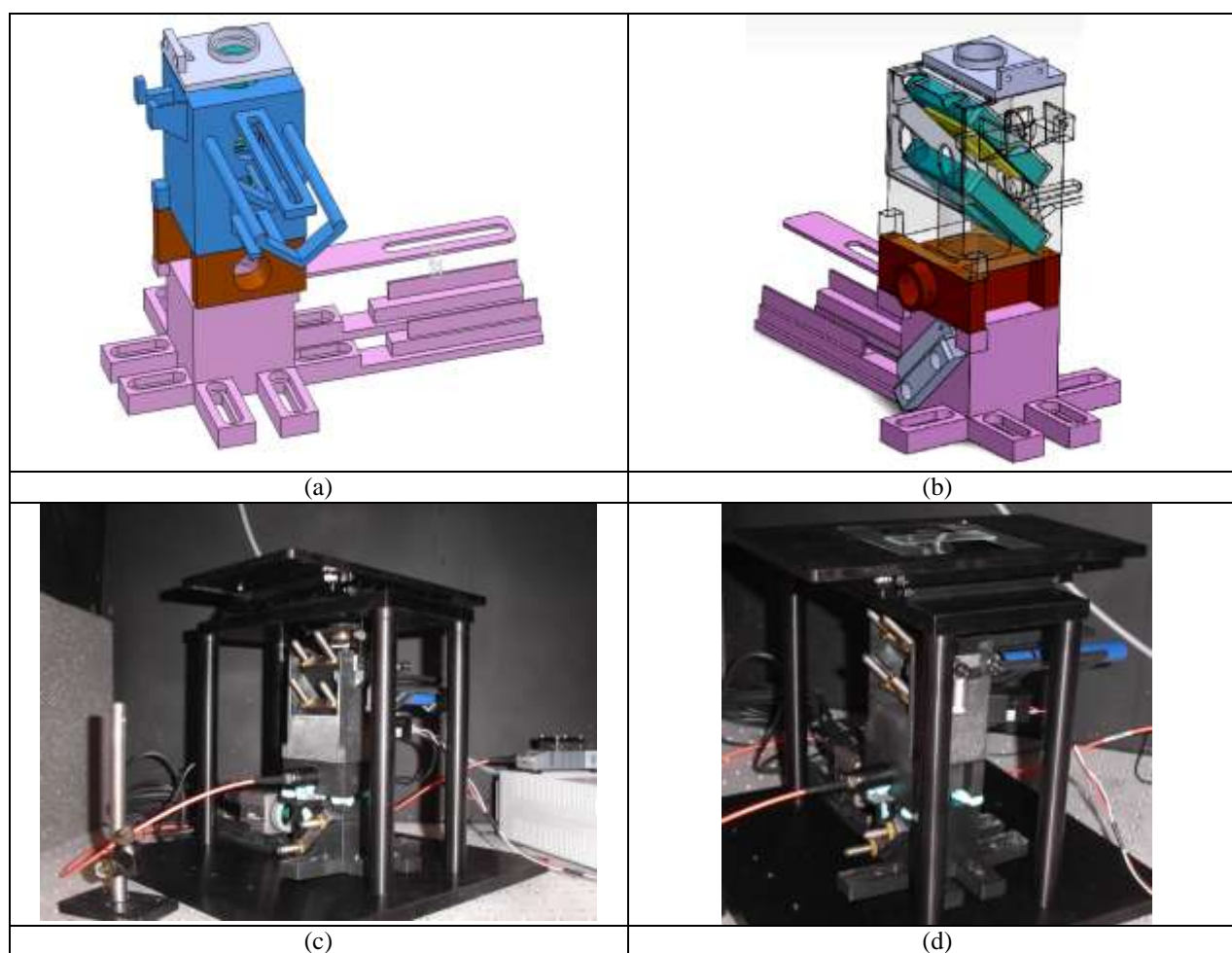
Fig. 2. Assembly of 3D-printed parts and optical/electronic parts. (a) and (b) are Solidworks drawing at two viewing angles to show the 3D-printed objective holder (grey), dichroic mirror holder (blue), beam splitter holder (brown) and holder for mirror and camera (purple). (c) and (d) are images showing the experimental set up that includes the 3D-printed plastic parts and associated optics and electronics as depicted in Figure 1. (c) reveals more clearly the camera, white light source with optical fiber (orange) and two dichroic mirrors; whereas (d) shows the chip, microscope objective and laser (blue) in a better viewing angle. The two dichroic mirrors and camera mirror are located on their respective mirror mounts with two thumb-adjustable screws.

monitoring system, the fluorescence drug's accumulation in single-cells could be quantified.

MATERIALS AND METHODS

Chip design
The layout of the microfluidic chip was designed using L-Edit (Tanners), and the chip design was sent to a printer (Coles Lithoprep) which produced the photomask on a plastic film. The microfluidic chip was made of polydimethylsiloxane (PDMS). As shown in the schematic diagram and image in Figure 3, the chip is composed of three channels, three reservoirs, and one chamber containing a cell retention structure. This chip was different from the ones described previously (Li *et al*., 2008; Li *et al*., 2011) in that it was made of polymeric plastics and it was simplified with two reservoirs less, making this new chip easier for the user to control the flow of reagents and capture the cells.

Reagents
Daunorubicin (DNR), calcein-AM ester (CaAM), cyclosporine A (CsA) and penicillin were obtained from Sigma-Aldrich (St Louis, MO). Fetal bovine serum (FBS) was obtained from ATCC (Manassas, VA). All reagents were of analytical grade.

Cell culture
Human ovarian carcinoma cell lines: NCI/ADR-RES and OVCAR-8 were generously provided by Michael M.

Gottesman of National Cancer Institute (NCI), USA. NCI/ADR-RES is an ovarian cell line, though its origin was previously mistaken as breast cancer (Ke *et al*., 2011). OVCAR-8 is the non-MDR parental control. All cell lines were cultured in RPMI 1460 medium supplemented with 10% fetal bovine serum, 2 mM L-glutamine, 100 I.U./mL penicillin, 100 μg/mL streptomycin in a 24-well cell culture plate (Greiner Bio One, Germany), and incubated at 37 °C and 5% CO_2. For cell passaging, confluent cells were washed with phosphate buffered saline (PBS) and incubated with 0.1% EDTA (Sigma) for detachment.

The single cell bioanalyzer (SCB)

The single cell bioanalyzer (SCB) was constructed by a microscope for optical imaging and fluorescence measurement of a cell, see Figure 1 and 2. The optical system (see Fig.1) has been employed for simultaneous fluorescence measurement and bright-field observation/imaging. The excitation light was provided by the blue laser, which was confirmed not to be critical to impact the cell membrane's permeability. The cell was captured in a microfluidic PDMS chip (Fig. 3). Figure 4 depicts the screenshots from the animation showing the principle of operation of the SCB. Briefly, when a group of cells is introduced into the single-cell chip, a desired cell is selected and retained near an arc slope opposite to a reagent channel of the chip. The cell's motion and selection was accomplished by using the hydrodynamic liquid flow. Reagents can be continuously delivered and switched. The measured voltage data were recorded by the Labview software. The cellular fluorescence intensity should be stable before the reagents were switched.
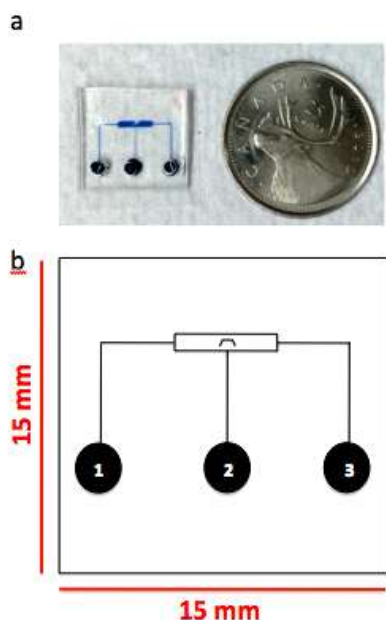

Fig. 3. The microfluidic chip consists of 3 solution reservoirs and 1 central chamber consisting of a cell retention structure. (a) The image shown a chip that is made of a 15mm×15mm (PDMS) slab that was sealed to a 0.17mm-thick glass slip. (b) The chip layout diagram shows the cell inlet reservoir 1, reagent reservoir 2, and waste reservoir 3 reach the microfluidic chamber that consists of a cell retention structure.

On-chip drug accumulation study on the same single cell

Calcein-AM ester (CaAM; λ_{ex}=470 nm; λ_{em}=535 nm) and daunorubicin (DNR; λ_{ex}=470 nm; λ_{em}=585 nm) were used as P-gp substrates for drug accumulation measurement.

Before use, the microfluidic chip was cleaned by LiquiNOX detergent, rinsed with purified water, and sterilized with 75% ethanol. When the cells were introduced from the left reservoir, they flowed from the left channel to the right. By adjusting the liquid levels of these reservoirs, a single cancer cell was led into the cell retention structure.

In order to identify DNR concentration in the cell, the effect of known amount of DNR standards were first tested in the cancer cell. After one cancer cell was selected and retained in the cell retention structure in the chip, cell media in all the reservoirs were removed, and then the drug inlet reservoir was filled with 5 μM DNR. Fluorescence measurement was started to monitor the increase in fluorescence intensity due to DNR accumulation in the cell. After the fluorescence intensity became stable, the procedure was repeated by treatment of the cell with DNR of higher concentrations (20, 35, 50, 65, and 80 μM). Since the fluorescence intensity was considered high enough at 35 μM, subsequent single-cell experiments were carried out at this DNR concentration.

For experiments, the key step was to measure the accumulation of the anticancer drug (i.e., DNR) in the absence and presence of the P-gp inhibitor, CsA. Different DNR concentrations were tested for measurements in the cell and outside the cell in the chip. To complete this function, the position of the chip was precisely controlled by a robotic arm to move the chip back and forth in three selected detection sites. Detection site 1 was on the PDMS chip wall; site 2 was focused on the chamber, in which the extracellular fluorescence intensity was detected; site 3 is on the cell, which provided the total fluorescence intensity. In principle, the fluorescence intensity from the PDMS chip wall should be zero. The fluorescence from detection site 2 was set as background. After deducting the background from the total fluorescence (measured from detection site 3), this corrected value was set to represent the amount of DNR accumulated in the cell.

RESULTS AND DISCUSSION

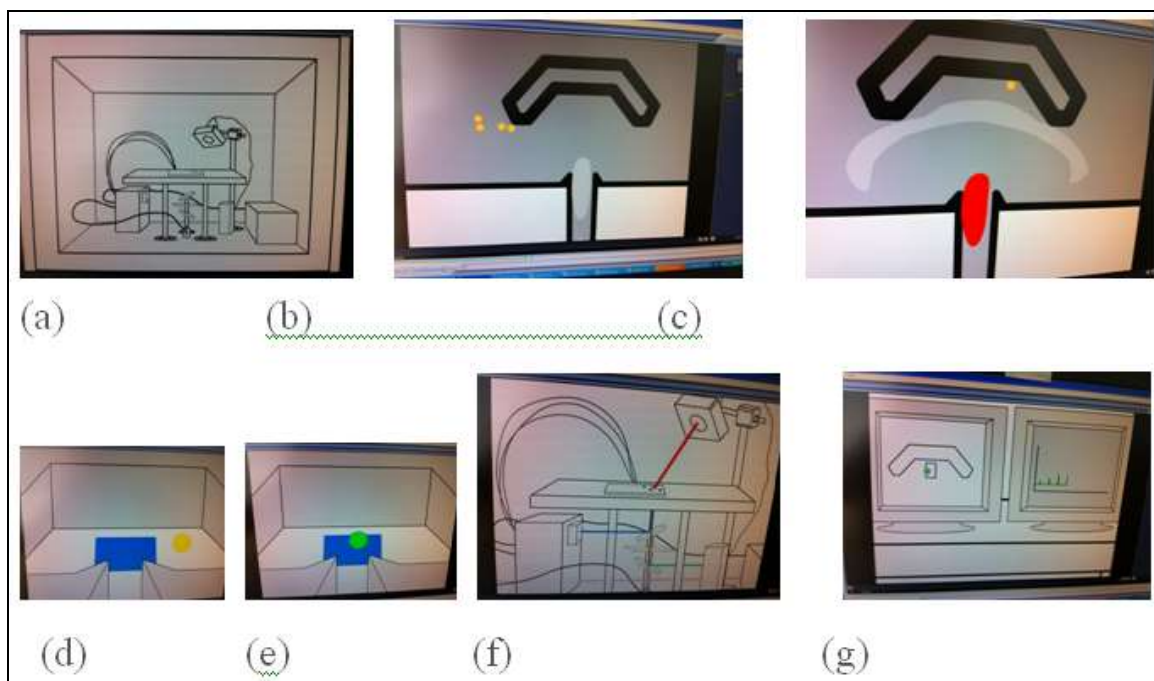After ovarian cancer cells are introduced in the cell inlet

Fig. 4. Screen-capture of an animation illustrating the principle of operation of the single cell bioanalyzer (SCB) instrument. (a) overview of SCB with a single-cell chip placed on the movable stage (b) a group of 4 cells (yellow) arrived at the cell retention structure in the chip (c) a single-cell (yellow) was selected in the microfluidic flow (in grey) and the flow of drug (in red) was delivered to the cell (d) the background was measured when the cell (yellow) was moved outside the excitation region (blue) (e) the cell with the drug became fluorescent (green) when it was moved inside the excitation region (blue) (f) simultaneous fluorescence measurement (green) and optical imaging (red) occurred (g) optical image was shown on the left computer screen and fluorescence measurement shown on the right. For the video chip of this animation, see supplementary information.

reservoir in the microfluidic chip, Figure 4 depicts how the cell is selected and captured in the chip, and how the SCB is used to conduct simultaneous optical imaging and fluorescence measurement of the captured cell in the chip. Briefly, when a group of cells is introduced into the single-cell chip, a desired cell is selected and retained in the cell retention structure opposite to a reagent channel of the chip. Then, reagents can be continuously delivered and switched to treat the cell, and fluorescence measurement data are being recorded by the Labview software.

Figure 5 indicates the measurement of CaAM accumulation in the OVCAR-8 single-cell which does not express P-gp. After CaAM ester entered the cell, it was hydrolyzed to generate calcein. While the cell and the surrounding background are measured successively, the peaks and baseline are recorded. The baseline indicates the extracellular CaAM and the peaks represent the accumulated calcein after it was formed in the OVCAR-8 cell. The peak heights continue to increase until saturation and this occurs without using any MDR modulator, indicating that efflux due to P-gp does not occur in the cell, and the cell is non-MDR.

On the other hand, a P-gp expressing cell such as NCI/ADR-RES was measured. Figure 6 a, b and c indicate the image of a single NCI/ADR-RES cell captured in the retention structure of the chip before experiment, during experiment and after experiment, respectively. No matter how long the chip was moved for how many times, detection site 3 should always measure the cell, and the positions of these sites should never change. The distance among these three sites is more than 10 μm but less than 50 μm. During a cycle of 120 s, the chip was consecutively moved to detection sites 1, 2 and 3 to complete the fluorescence measurement on the PDMS background, outside the cell, and in the cell, respectively. We have demonstrated that the single-cell chip should have a wide and flat region for effective cell scanning and successful background correction.

The effect of cyclosporine A (CsA) on cancer cells in the SCB was determined. After one ovarian cancer cell was captured in the retention structure, the cell media in all the reservoirs were removed, and then the cell was first treated with DNR (35 μM) in the absence of CsA for about 1400 s for drug accumulation (control). Thereafter, the same cell was treated with a solution of 35 μM DNR
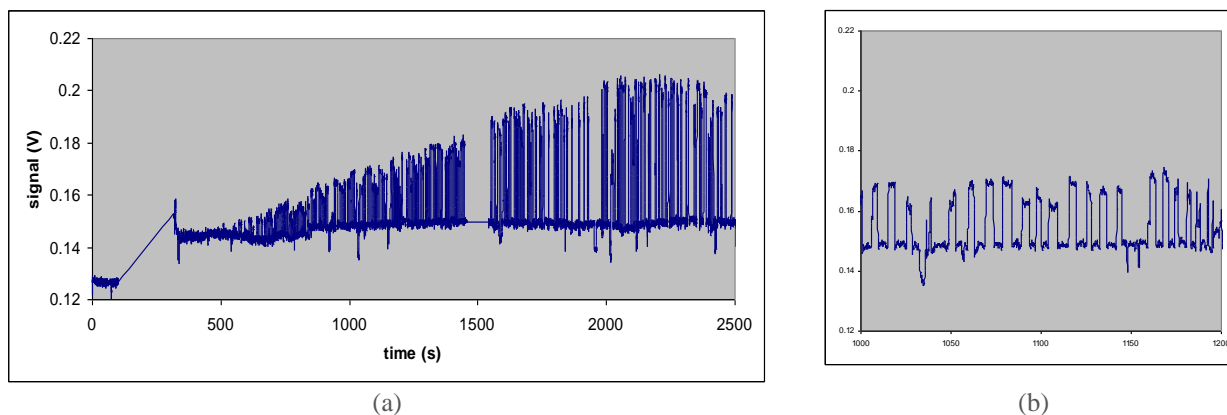
(a)   (b)

Fig. 5. Measurement of a single non-MDR OVCAR-8 cell when calcein-AM (CaAM, 1 μM) is being accumulated. (a) fluorescence signal plotted against time, with DNR (35 μM) added (at 140 s); (b) expansion of graph in (a) during 1000-1200 s, showing the peaks (total fluorescence) and baseline (background interference due to extracellular DNR). The peaks keep increasing to a plateau when calcein is being accumulated in the non-MDR cell until saturation.

Fig. 6. Images of one P-gp expressing ovarian cancer cell (NCI/ADR-RES) retained in the cell retention structure of a microfluidic chip (a) after DNR (35 μM) was added (at 200 s); (b) after CsA (5 μM) together with DNR (35 μM) were added (at 1400 s); (c) after trypan blue was introduced to treat the cell when the test ended (at 3400 s). After CsA was added together with DNR, the cell turns brightly fluorescent (b), and since the cell was not stained after the test (c), it was still viable after measurement. The times listed can be referred to in Figure 7 which depicts the measurement data. The scale was marked on the screen for cell size measurement, with the smallest graduation indicating 10 μm.

containing 5 μM CsA (experiment). As the modulator has a positive effect, a higher drug accumulation is observed instantly; this enhancement is depicted as a bright cell in Figure 6 b and a high transition in the correction signal in Figure 7. It means that with the help of CsA, more DNR is accumulated in the cell than its control. From the corrected signal in Figure 7, the intracellular DNR concentration of the single NCI/ADR-RES cell was determined to increase by 3 folds against its same-cell control, i.e. 0.025/0.008 = 3.

The observation of CsA in enhancing the DNR accumulation was consistent with our previous studies by SASCA (same-single-cell analysis). With every test cell having two identities, one is the test cell, and the other is its same-cell control, this method allows background correction, which remove interference, essentially eliminating the effect of electrical noise and extracellular solution fluctuations.

This SCB instrument had completed the imaging analysis with simultaneous DNR accumulation measurement, and it also showed the effectiveness of MDR modulation by CsA, overcoming MDR in ovarian cells. Moreover, the collection of time-dependent fluorescence data can help understand the kinetics of drug accumulation in MDR cancer cells, without long-time and tedious tissue culture conducted conventionally.

CONCLUSION

In this study, it is found that the SCB is useful for the measurement of cellular fluorescence, which is unaffected by the presence of reagent switch and buffer fluctuations. Such a single-cell fluorescence measurement may have a potential to provide information about the response of ovarian cancer patient cells to chemotherapeutic drugs.
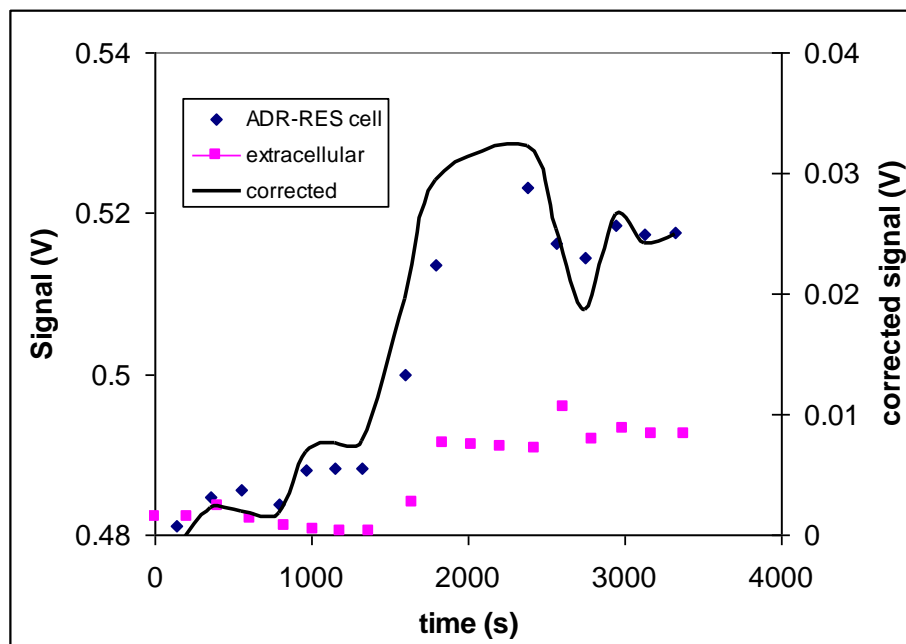
Fig. 7. DNR accumulation measured in a single P-gp expressing ovarian cancer cell (NCI/ADR-RES). The fluorescence intensity of DNR during its accumulation in the cell is plotted against time. At 1400 s, CsA (5 μM) together with DNR were added in the chip. Blue dots indicate the fluorescence intensity due to intracellular DNR, and pink dots represent the fluorescence intensity of extracellular DNR. The blue dots reach the first plateau at about 0.48 V after 1000 s and the second one at about 0.51 V after 3000 s. The corrected signal, which is obtained by subtracting the pink dots from the blue dots, is depicted as a black line, showing 0.008 V at 1300 s, and 0.025 V at 3300 s. The fold increase of DNR accumulation enhancement due to CsA is estimated by 0.025/0.008 = 3.

ACKNOWLEDGEMENTS

REFERENCES

Chen, YC., Kolesnyk, I., Li, PCH., Yue, PYK. and Wong, RNS. 2014. Microfluidic Single Cell Bioanalysis to measure drug uptake on single multidrug resistant cancer cell as enhanced by ginsenoside Rg 3. Proceedings of Science Plus International Conference, Nov. 14-15, 2014, Hong Kong. pp. 5-7.

El-Ali, J., Sorger, PK. and Jensen, KF. 2006. Cells on chips. Nature. 442(27):403-411.

Gómez-Sjöberg R., Leyrat AA., Pirone, DM., Chen, CS. and Quake, SR. 2007. Versatile, Fully Automated, Microfluidic Cell Culture System. Anal. Chem. 79(22):8557-63.

Halldorsson, S., Lucumi, E., Gmez-Sjberg, R. and Fleming, RMT. 2015. Advantages and challenges of microfluidic cell culture in polydimethylsiloxane devices. Biosens. Bioelectron., 63:218-231.

Ke, W., Yu, P., Wang, J., Wang, R., Guo, C., Zhou, L., Li, C. and Li, K. 2011. MCF-7/ADR cells (re-designated NCI/ADR-RES) are not derived from MCF-7 breast cancer cells: a loss for breast cancer multidrug-resistant research. Med. Oncol. Suppl 1:S135-41.

Khamenehfar, A., Wang, HY., Li, PCH., Schmidt, C. and Lopez, A. 2014[a]. Drug resistance of a single mouse melanoma cell and its interaction with a mouse dendritic cell studied using the microfluidic single cell bioanalyzer. 6th International Symposium on Microchemistry and Microsystems, Jul 30-Aug 1, Singapore. pp. 1-2.

Khamenehfar, A., Wan, CPL., Li, PCH., Letchford, K. and Burt, HM. 2014[b]. Same-single-cell analysis using the microfluidic biochip to reveal drug accumulation enhancement by an amphiphilic diblock copolymer drug formulation. Anal. Bioanal. Chem. 406:7071-7083.

Khamenehfar, A., Beischlag, TV., Russel, P., Ling, P., Nelson, C. and Li, PCH. 2015[a]. Label-free Isolation of a Prostate Cancer Cell among Blood Cells and the Single-Cell Measurement of Drug Accumulation Using an Integrated Microfluidic Chip. Biomicrofluidics. 9, 064104:1-18.

Khamenehfar, A., Li, PCH. and Leung, ELH. 2015[b]. Gefitinib enhanced cancer drug uptake in the same single non-small cell lung cancer cells observed in real-time in the microfluidic biochip. 2nd International Biotechnology, Chemical Engineering & Life Science Conference, July 20-22, 2015, Hokkaido, Japan. pp. 1-3.

Khamenehfar, A., Maher G., Chen, YC., Donna, H. and Li, PCH. 2016. Dielectrophoretic Microfluidic Chip Enables Single-Cell Measurements for Multidrug Resistance in Heterogeneous Acute Myeloid Leukemia Patient Samples. Anal. Chem. 88:5680-5688.

Li, XJ., Ling, V. and Li, PCH. 2008. Same-single-cell analysis for the study of drug efflux modulation of multidrug resistant cells using a microfluidic chip. Anal. Chem. 80:4095-4102.

Li, XJ., Chen, YC. and Li, PCH. 2011. A simple and fast microfluidic approach of same-single-cell analysis (SASCA) for the study of multidrug resistance modulation in cancer cells. Lab Chip. 11:1378-84.

Li, W., Zhang, H., Assaraf, YG., Zhao, K., Xu, X., Xie, J., Yang, D. and Chen, Z. 2016. Overcoming ABC transporter-mediated multidrug resistance: Molecular mechanisms and novel therapeutic drug strategies. Drug Resistance Updates. 27:14-29.

Lindström, S. and Andersson-Svahn, H. 2010. Overview of single-cell analyses: microdevices and applications. Lab Chip. 10(24):3363-72.

Marquez, B. and Van Bambek, F. 2011. ABC multidrug transporters: target for modulation of drug pharmacokinetics and drug–drug interactions. Curr. Drug Targets. 12:600-620.

Sharom, FJ. 2008. ABC multidrug transporters: structure, function, and role in chemoresistance. Pharmacogenomics. 9(1):105-127.

Peng, XY. and Li, PCH. 2005. Extraction of pure cellular fluorescence by cell scanning in a single-cell microchip. Lab Chip. 5:1298-1302.

Thomas, H. and Coley HM. 2003. Overcoming multidrug resistance in cancer: an update on the clinical strategy of inhibiting p-glycoprotein. Cancer Control. 10(2):159-165.